ISSN 0021-3640, JETP Letters, 2006, Vol. 83, No. 9, pp. 418–422. © Pleiades Publishing, Inc., 2006.

Superconducting Decay Length in a Ferromagnetic Metal¶

D. Yu. Gusakova[a], A. A. Golubov[b], and M. Yu. Kupriyanov[a]
[a] *Institute of Nuclear Physics, Moscow State University, Moscow, 119992 Russia*
e-mail: dariamessage@yandex.ru
[b] *Faculty of Science and Technology, University of Twente, 7500 AE Enschede, The Netherlands*
Received April 6, 2006

The complex decay length ξ characterizing the penetration of superconducting correlations into a ferromagnet due to the proximity effect is studied theoretically in the framework of the linearized Eilenberger equations. The real part ξ_1 and imaginary part ξ_2 of the decay length are calculated as functions of exchange energy and the rates of ordinary, spin-flip, and spin–orbit electronic scattering in a ferromagnet. The lengths $\xi_{1,2}$ determine the spatial scales of, respectively, the decay and oscillation of a critical current in SFS Josephson junctions in the limit of a large distance between superconducting electrodes. The developed theory provides the criteria of applicability of the expressions for ξ_1 and ξ_2 in the dirty and clean limits, which are commonly used in the analysis of SF hybrid structures.

PACS numbers: 74.50.+r, 74.80.Dm, 75.30.Et
DOI: 10.1134/S0021364006090116

The decay length ξ is an important material parameter which characterizes the scale of penetration of superconducting correlation into a non-superconducting material across an interface with a superconductor. The critical current I_C in a Josephson junction scales exponentially with the distance between the superconducting electrodes L if L is larger than ξ: $I_C \propto \exp\{-L/\xi\}$. In nonmagnetic materials, the decay length is a real number, while in ferromagnets ξ is a complex number (see [1–4] for reviews). In particular, if the condition of the so-called dirty limit is fulfilled in the F metal, the decay length is

$$\xi^{-1} = \xi_1^{-1} + i\xi_2^{-1}, \quad \xi_{1,2}^{-1} = \sqrt{\frac{\sqrt{(\pi T)^2 + H^2} \pm \pi T}{D_F}}, \quad (1)$$

where D_F and H are the diffusive coefficient and the exchange field in a ferromagnet, respectively. In the clean limit,

$$\xi_1^{-1} = \xi_0^{-1} + l^{-1}, \quad \xi_0^{-1} = \frac{2\pi T}{v_F},$$
$$\xi_2^{-1} = \xi_H^{-1} = \frac{2H}{v_F}, \quad (2)$$

where v_F is the Fermi velocity in a ferromagnet and l is the electron mean free path. From (1) and (2) it is clearly seen that for dirty materials $\xi_2 > \xi_1$, and, in the limit of large $H \gg \pi T$, the characteristic lengths are nearly equal, $\xi_1 \approx \xi_2$. In the clean limit, length scales ξ_1 and ξ_2 are completely independent.

¶ The text was submitted by the authors in English.

The existing experimental data obtained up to now in SFS Josephson junctions [5–16] can be separated into two groups depending on whether a weak or a strong ferromagnet was used for junction fabrication. To be considered as a weak ferromagnet, the dilute ferromagnetic alloys (e.g., $Cu_{1-x}Ni_x$) should be in the range of concentration close to the critical one ($x \approx 0.5$). The electron mean free path in these alloys is very small, fulfilling the conditions of the dirty limit. As a result, the observed relation between the decay (ξ_1) and oscillation (ξ_2) lengths, $\xi_2 \gtrsim \xi_1$, is close to that following from (1). It is necessary to point out that, in some experiments [12], the observed difference between ξ_2 and ξ_1 is so large that it cannot be explained by the temperature factor in (1) only, and spin-dependent scattering processes should be taken into account [12, 17].

In contrast, in structures with a strong ferromagnet [11, 16] (Ni, Ni_3Al), the relation between ξ_1 and ξ_2 is just the opposite, and a large ratio $\xi_1/\xi_2 \sim 10$ was observed in Ni_3Al [16]. Therefore, a more complex model should be developed for the data's interpretation.

Most previous theoretical work on SF hybrids was performed assuming the dirty limit (see [2–4]), and only first-order corrections to the decay length in the small parameter $l\xi_H \ll 1$ were discussed in [18–20]. Some solutions in the clean and intermediate regimes were obtained in a number of works, e.g., [21–24], but were not analyzed in detail. The purpose of this work is to develop general theory describing the decay length ξ in a ferromagnet for any relation between ξ_0, ξ_H, and l.

To do this, we consider a generic SFS Josephson junction with arbitrary transparency of SF interfaces and a large thickness of the F layer, $L \gg \xi_1$. It is well known [1–4] that the critical current of this structure should fall exponentially with L,

$$I_C = I_0 \exp\{-L/\xi\}.$$

Here, the prefactor I_0 depends on the physical properties of SF interfaces and the nearby S and F regions, while ξ depends only on the bulk parameters of F material and can be obtained [25, 26] as the solution of linearized quasi-classical Eilenberger equations [27]. These equations are valid at distances from the interfaces larger than ξ and have the form [27, 3, 4]

$$(\xi_0^{-1} \pm i\xi_H^{-1})f_\pm + \cos\theta \frac{\partial}{\partial x} f_\pm = l_{\text{eff}}^{-1}(\langle f_\pm\rangle - f_\pm) + l_{\text{soeff}}^{-1}(f_\mp - f_\pm), \tag{3}$$

$$l_{\text{eff}}^{-1} = l^{-1} + l_z^{-1} + 2l_x^{-1}, \tag{4}$$

$$l_{\text{soeff}}^{-1} = l_{\text{so}}^{-1} - l_x^{-1}, \quad \langle\ldots\rangle = \int_0^\pi (\ldots)\sin\theta d\theta. \tag{5}$$

Here, θ is the angle between the direction of electron velocity v_F and the x axis, which is oriented perpendicular to the interfaces; $f_\pm = f_\pm(x, \theta)$ are the quasi-classical Eilenberger functions describing the behavior of spin-up and spin-down electrons in the presence of the exchange field H oriented parallel to the SF interfaces. The parameters $l_{\text{so}} = v_F\tau_{\text{so}}$ and $l_z = v_F\tau_z$, $l_x = v_F\tau_x$ are the electron mean free paths for magnetic scattering parallel and perpendicular to the direction of H, while $l_{\text{so}} = v_F\tau_{\text{so}}$ is the electron mean free path for the spin–orbit interaction.

The solution of Eq. (3) has the form

$$f_\pm(x, \theta) = C_\pm(\theta)\exp\left\{-\frac{x}{\xi}\right\}, \quad \xi^{-1} = \xi_1^{-1} + i\xi_2^{-1}, \tag{6}$$

where ξ is the effective decay length independent of θ. Substitution of (6) into (3) yields a system of two equations for $C_\pm(\theta)$:

$$(\xi_0^{-1} + i\xi_H^{-1})C_+(\theta) - \xi^{-1}\cos\theta C_+(\theta) = l_{\text{eff}}^{-1}(\langle C_+(\theta)\rangle - C_+(\theta)) + l_{\text{soeff}}^{-1}(C_-(\theta) - C_+(\theta)), \tag{7}$$

$$(\xi_0^{-1} - i\xi_H^{-1})C_-(\theta) - \xi^{-1}\cos\theta C_-(\theta) = l_{\text{eff}}^{-1}(\langle C_-(\theta)\rangle - C_-(\theta)) + l_{\text{soeff}}^{-1}(C_+(\theta) - C_-(\theta)). \tag{8}$$

The solution of these equations has the form

$$C_+(\theta) = \frac{\langle C_+(\theta)\rangle\Lambda_-^{-1} + l_{\text{soeff}}^{-1}\langle C_-(\theta)\rangle}{l_{\text{eff}}(\Lambda_+^{-1}\Lambda_-^{-1} - l_{\text{soeff}}^{-2})}, \tag{9}$$

$$C_-(\theta) = \frac{\langle C_-(\theta)\rangle\Lambda_+^{-1} + l_{\text{soeff}}^{-1}\langle C_+(\theta)\rangle}{l_{\text{eff}}(\Lambda_+^{-1}\Lambda_-^{-1} - l_{\text{soeff}}^{-2})}, \tag{10}$$

$$\xi_{10}^{-1} = \xi_0^{-1} + l_{\text{eff}}^{-1} + l_{\text{soeff}}^{-1},$$

$$\Lambda_\pm^{-1} = \xi_{10}^{-1} - \xi^{-1}\cos\theta \pm i\xi_H^{-1}.$$

Averaging in (9) and (10) over the angle θ, we get a system of two equations for $\langle C_\pm(\theta)\rangle$. Its compatibility condition results in the equation for the effective decay length ξ_{eff}:

$$\tanh\frac{\xi^{-1}}{l_{\text{eff}}^{-1}} = \frac{\xi^{-1}}{\xi_{10}^{-1} \pm \sqrt{(l_{\text{soeff}}^{-2} - \xi_H^{-2})}}. \tag{11}$$

It is clearly seen that, if the effective spin–orbit interaction is so strong that $l_{\text{soeff}}^{-1} \geq \xi_H^{-1}$, then the right-hand side of (11) is real. Therefore, in this case Eq. (11) provides us with two solutions for ξ_1^{-1}, while $\xi_2^{-1} = 0$. It is necessary to mention that, in the absence of ferromagnetic ordering ($H = 0$) due to degeneracy in the spin orientation, the critical current must not depend on l_{soeff}. In this situation, only the root of the equation corresponding to the "+" sign in Eq. (11) should be considered,

$$\tanh\frac{\xi_{11}^{-1}}{l_{\text{eff}}^{-1}} = \frac{\xi_{11}^{-1}}{\xi_0^{-1} + l_{\text{eff}}^{-1}}, \tag{12}$$

which provides the largest value of the decay length. The solution of Eq. (11),

$$\tanh\frac{\xi_{12}^{-1}}{l_{\text{eff}}^{-1}} = \frac{\xi_{12}^{-1}}{\xi_0^{-1} + l_{\text{eff}}^{-1} + 2l_{\text{soeff}}^{-1}}, \tag{13}$$

with the smaller $\xi = \xi_{12}$, also exists at finite H. (In the limit $H \longrightarrow 0$, the prefactor before this exponential solution goes to zero [17], making the critical current independent of ξ_{12}.) At $l_{\text{soeff}} = \xi_H$, these two lengths are equal to each other, $\xi_{11} = \xi_{12}$. With a further increase in H, the right-hand side of Eq. (11) becomes complex, and Eq. (11) can be rewritten as

$$\tanh\frac{\xi^{-1}}{l_{\text{eff}}^{-1}} = \frac{\xi^{-1}}{\xi_{10}^{-1} + i\xi_{20}^{-1}}, \quad \xi_{20}^{-1} = \sqrt{\xi_H^{-2} - l_{\text{soeff}}^{-2}}. \tag{14}$$

The sign "–" in Eq. (11) simply provides the equation for the complex-conjugate solution of Eq. (14).

In the limit $l_{\text{eff}} \ll \xi$, one can expand the hyperbolic tangent in (14) in series, keeping the first three terms, and get

$$\frac{l_{\text{eff}}}{\xi_1} = \sqrt{\frac{3\Gamma_+}{2}}\left[1 + \frac{1}{10}\left(\frac{l_{\text{eff}}}{\xi_{01}} - 1 - \frac{l_{\text{eff}}^2}{\xi_{20}^2\Gamma_+}\right)\right], \tag{15}$$

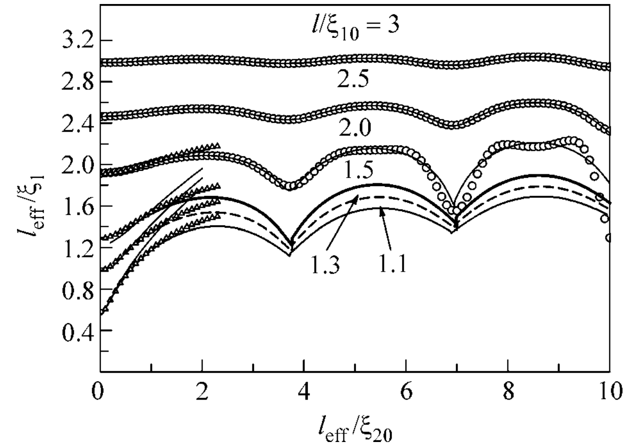

Fig. 1. Decay length ξ_1^{-1} vs. ξ_{20}^{-1} calculated for different values of ξ_{10}^{-1}. The open circles are the asymptotic curves calculated from (20) for ξ_{10}^{-1} = 2, 2.5 and 3. The open triangles are the asymptotic curves calculated from (15) for ξ_{10}^{-1} = 1.1, 1.3, 1.5, and 2. The thin solid lines are the asymptotic dependences following from Eq. (15) without the correction in the square brackets. These curves are calculated for ξ_{10}^{-1} = 1.1, 1.3, and 1.5.

$$\frac{l_{\text{eff}}}{\xi_2} = \sqrt{\frac{3\Gamma_-}{2}}\left[1+\frac{1}{10}\left(\frac{l_{\text{eff}}}{\xi_{01}}-1+\Gamma_+\right)\right],$$
$$\Gamma_\pm = \sqrt{\left(\frac{l_{\text{eff}}}{\xi_{01}}-1\right)^2+\frac{l_{\text{eff}}^2}{\xi_{20}^2}} \pm \left(\frac{l_{\text{eff}}}{\xi_{01}}-1\right). \tag{16}$$

The expressions in the square brackets in (15) and (16) give first-order corrections to the dirty limit formula [17] for ξ_1 and ξ_2. This approximation is valid if

$$\sqrt{\xi_0^{-2}+2\xi_0^{-1}l_{\text{soeff}}^{-1}+\xi_H^{-2}} \pm (\xi_0^{-1}+l_{\text{soeff}}^{-1}) \ll l_{\text{eff}}^{-1}. \tag{17}$$

In the limit ξ_0, $l_{\text{soeff}} \gg \xi_H$, the expression $\xi = \sqrt{\frac{D_F}{iH}\left(1-\frac{2}{5}iH\tau\right)}$, $\tau = l/v_F$ follows from Eqs. (15) and (16). This formula was obtained earlier in [18, 19] and can be interpreted as a complex correction to the diffusion coefficient, $D_F^{\text{eff}} = D_F\left(1-\frac{2}{5}iH\tau\right)$.

In the clean limit,

$$A \gg \max\left\{\ln\sqrt{A},\ \ln\sqrt[4]{\frac{l_{\text{eff}}^2}{\xi_H^2}-\frac{l_{\text{eff}}^2}{l_{\text{soeff}}^2}}\right\},$$
$$A = 1+\frac{l_{\text{eff}}}{\xi_0}+\frac{l_{\text{eff}}}{l_{\text{soeff}}}. \tag{18}$$

In the first approximation, we may set the hyperbolic tangent in (14) equal to unity and get

$$\xi_1^{-1} = \xi_{10}^{-1}, \quad \xi_2^{-1} = \xi_{20}^{-1}. \tag{19}$$

It is clearly seen that, for $l_{\text{soeff}}^{-1} \longrightarrow 0$, this formula transforms into Eq. (2). In the next approximation, it is easy to find that the corrections to (19),

$$\xi_1^{-1} = \xi_{10}^{-1} - 2p\exp\left(-\frac{2l_{\text{eff}}}{\xi_{10}}\right), \tag{20}$$

$$\xi_2^{-1} = \xi_{20}^{-1} + 2q\exp\left(-\frac{2l_{\text{eff}}}{\xi_{10}}\right), \tag{21}$$

where

$$p = \xi_{20}^{-1}\sin\left(\frac{2l_{\text{eff}}}{\xi_{20}}\right)+\xi_{10}^{-1}\cos\left(\frac{2l_{\text{eff}}}{\xi_{20}}\right),$$

$$q = \xi_{10}^{-1}\sin\left(\frac{2l_{\text{eff}}}{\xi_{20}}\right)-\xi_{20}^{-1}\cos\left(\frac{2l_{\text{eff}}}{\xi_{20}}\right)$$

are oscillating functions of ξ_H.

Equation (14) is equivalent to the system of equations for ξ_1 and ξ_2:

$$\frac{\xi_1^{-1}}{\xi_{10}^{-1}} = \coth\frac{2\xi_1^{-1}}{l_{\text{eff}}^{-1}} - a\cos\left(\frac{2\xi_2^{-1}}{l_{\text{eff}}^{-1}} - \arctan\frac{\xi_2^{-1}}{\xi_{10}^{-1}}\right), \tag{22}$$

$$\frac{\xi_2^{-1}}{\xi_{20}^{-1}} = \coth\frac{2\xi_1^{-1}}{l_{\text{eff}}^{-1}} - b\cos\left(\frac{2\xi_2^{-1}}{l_{\text{eff}}^{-1}} + \arctan\frac{\xi_1^{-1}}{\xi_{20}^{-1}}\right), \tag{23}$$

$$a = \frac{\sqrt{\xi_{10}^{-2}+\xi_2^{-2}}}{\xi_{10}^{-1}\sinh(2\xi_1^{-1}/l_{\text{eff}}^{-1})}, \quad b = \frac{\sqrt{\xi_{20}^{-2}+\xi_1^{-2}}}{\xi_{20}^{-1}\sinh(2\xi_1^{-1}/l_{\text{eff}}^{-1})}.$$

From the structure of equations (22) and (23), it follows that an increase in ξ_{20}^{-1} leads to an increase in ξ_2^{-1}. This, in turn, results in an increase in the second negative item on the right-hand side of (22). Since ξ_1^{-1} must be a positive value, the increase in ξ_2^{-1} should be accompanied by a jump at a certain point to the positive branch of $\cos(x)$, leading to a discontinuity of the $\xi_2^{-1}(\xi_{20}^{-1})$ dependence. This consideration is proved by the numerical solution of (14) (see Figs. 1–3).

Figures 1 and 2 show the dependences of $\xi_1^{-1}(\xi_{20}^{-1})$ and $\xi_2^{-1}(\xi_{20}^{-1}) - \xi_{20}^{-1}$ calculated for fixed values of the parameter ξ_{10}^{-1}. Open triangles and circles in the figures show the asymptotic dependences (15), (16) and (20), (21), respectively. It is clearly seen that, in the parameter intervals $\xi_{20}^{-1} \le 10l_{\text{eff}}^{-1}$, $\xi_{10}^{-1} \ge 2l_{\text{eff}}^{-1}$, expressions (20) and (21) provide a good fit to the exact solution of

Eq. (14). The dirty limit formulas (15) and (16) are valid up to $\xi_{20}^{-1} \le 2l_{\rm eff}^{-1}$ for $\xi_{10}^{-1} \le 2l_{\rm eff}^{-1}$. Figure 3 gives the ratio ξ_2/ξ_1 as a function of ξ_{20}^{-1} for a set of $l_{\rm eff}/\xi_{10}$. At $H \longrightarrow 0$, the oscillation length ξ_2 goes to infinity. Therefore, the ratio diverges at $\xi_{20}^{-1} \longrightarrow 0$. With an increase in H, the ratio rapidly decreases, approaching the law $\xi_2/\xi_1 \propto \xi_{20}^{-1}$ at $\xi_{20}^{-1} \ge 2$.

The discovered behavior of ξ_2 and ξ_1 is quite general and must also be observed in structures without ferromagnetic ordering. An example is a normal filament of finite length, which is placed between superconducting banks and is biased by a dc supercurrent. It was shown [28], the minigap induced in this filament from the S electrodes is not a monotonic function of the phase difference across the structure. This behavior could also be explained in terms of the specific dependences of ξ_2 and ξ_1 upon the electron mean free path in current-biased systems.

In summary, by solving the linearized Eilenberger equations, we have calculated the real, ξ_1, and the imaginary, ξ_2, part of a decay length as a function of the exchange energy H and the mean free paths l, $l_{\rm so}$, l_z, and l_x for ordinary, spin-orbit, and spin-flip electronic scattering in a ferromagnet. These parameters, ξ_1 and ξ_2, characterize the penetration of superconducting correlations into a ferromagnet due to the proximity effect and determine the decay and oscillation lengths of the critical current in long SFS Josephson structures. We have found the range of validity of expressions (1) and (2), which are commonly used for interpretation of experimental data. In particular, the dirty limit expressions (1) are valid if $\xi_{20}^{-1} \le 0.5l_{\rm eff}^{-1}$ for $\xi_{10}^{-1} \le 0.5l_{\rm eff}^{-1}$. The corrected expressions (15) and (16) can be used in a broader range of $\xi_{20}^{-1} \le 2l_{\rm eff}^{-1}$ and $\xi_{10}^{-1} \le 2l_{\rm eff}^{-1}$. A further increase in the exchange field makes the length ξ_2 smaller than $l_{\rm eff}$, thus breaking down the validity of approximations used in the derivation of the Usadel equations. It is interesting to note that, in a certain parameter range, jumps occur in the dependence of ξ_2 vs. ξ_{20}, while ξ_1 remains a continuous function of ξ_{20}.

We have also demonstrated that intuitive knowledge about the relation between ξ_1 and ξ_2, based on the dirty limit theory, has a very limited range of applicability and cannot be used for $\xi_H > 5l$ or for $H\tau > 0.1$. In particular, an increase in H is not always accompanied by a decrease in ξ_1, and in a certain parameter range ξ_1 may even increase with H. The fact that one may reasonably combine a large decay length with the smaller period of oscillations looks rather attractive for possible applications of SFS Josephson junctions.

We are grateful to A.D. Zaikin, L. Tagirov, and A. Buzdin for useful discussions. This work was supported in part by the European Science Foundation (PI-Shift Program), the Russian Foundation for Basic Research (project no. 06-02-90865), and the NanoNed Program (project no. TCS 7029).

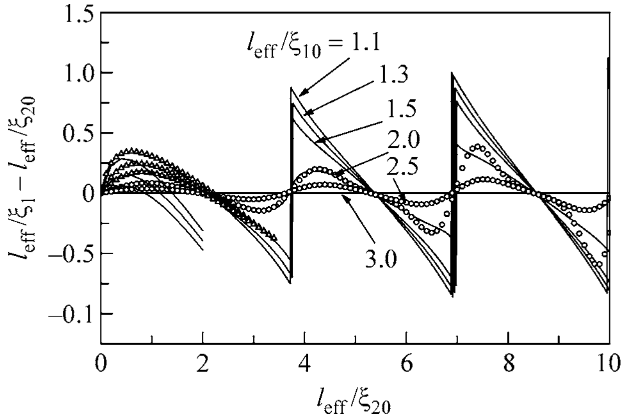

Fig. 2. Difference between the decay lengths ξ_2^{-1} and ξ_{20}^{-1} vs. ξ_{20}^{-1} calculated for different values of ξ_{10}^{-1} shown in the figure. The open circles are the asymptotic curves calculated from (21) for ξ_{10}^{-1} = 2, 2.5, and 3. The open triangles are the asymptotic curves calculated from (16) for ξ_{10}^{-1} = 1.1, 1.3, 1.5, and 2. The thin solid lines are the asymptotic dependences following from Eq. (16) without the correction in the square brackets. These curves are calculated for ξ_{10}^{-1} = 1.1, 1.3, and 1.5.

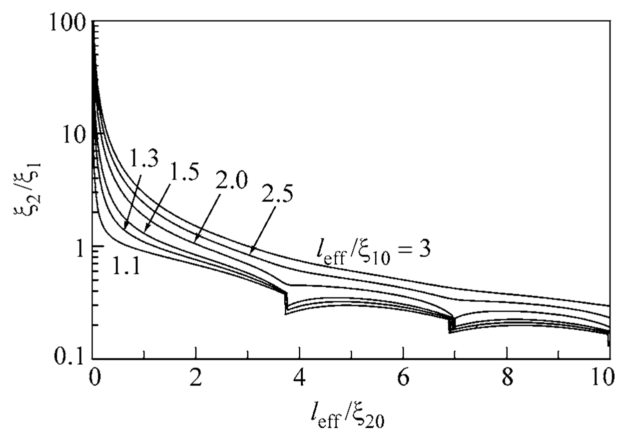

Fig. 3. Ratio of oscillation and decay lengths ξ_2/ξ_1 as a function of ξ_{20}^{-1} calculated for different values of ξ_{10}^{-1}.

REFERENCES

1. K. K. Likharev, Rev. Mod. Phys. **51**, 101 (1979).
2. A. A. Golubov, M. Yu. Kupriyanov, and E. Il'ichev, Rev. Mod. Phys. **76**, 411 (2004).
3. A. I. Buzdin, Rev. Mod. Phys. **77**, 935 (2005).

4. F. S. Bergeret, A. F. Volkov, and K. B. Efetov, Rev. Mod. Phys. **77**, 1321 (2005).
5. V. V. Ryazanov, V. A. Oboznov, A. Yu. Rusanov, et al., Phys. Rev. Lett. **86**, 2427 (2001).
6. T. Kontos, M. Aprili, J. Lesueur, et al., Phys. Rev. Lett. **89**, 137007 (2002).
7. H. Sellier, C. Baraduc, F. Lefloch, and R. Calemczuck, Phys. Rev. B **68**, 054531 (2003).
8. Y. Blum, A. Tsukernik, M. Karpovski, et al., Phys. Rev. B **70**, 214501 (2004).
9. C. Surgers, T. Hoss, C. Schonenberger, et al., J. Magn. Magn. Mater. **240**, 598 (2002).
10. C. Bell, R. Loloee, G. Burnell, and M. G. Blamire, Phys. Rev. B **71**, 180501 (R) (2005).
11. V. Shelukhin, A. Tsukernik, M. Karpovski, et al., cond-mat/0512593.
12. V. A. Oboznov, V. V. Bol'ginov, A. K. Feofanov, et al., cond-mat/0508573.
13. M. Weides, K. Tillmann, and H. Kohlstedt, cond-mat/0511546; M. Weides, M. Kemmler, E. Goldobin, et al., cond-mat/0604097.
14. H. Sellier, C. Baraduc, F. Lefloch, and R. Calemczuck, Phys. Rev. Lett. **92**, 257005 (2004).
15. M. Yu. Kupriyanov, A. A. Golubov, and M. Siegel, Proc. SPIE (2006) (in press).
16. F. Born, M. Siegel, E. K. Hollmann, et al., submitted to Phys. Rev. B.
17. M. Fauré, A. I. Buzdin, A. A. Golubov, and M. Yu. Kupriyanov, Phys. Rev. B **73**, 064505 (2006).
18. A. I. Buzdin and I. Baladie, Phys. Rev. B **67**, 224514 (2003).
19. L. Tagirov, Physica C (Amsterdam) **307**, 145 (1998); private communication.
20. Ya. V. Fominov, M. Yu. Kupriyanov, and M. V. Feigel'man, Usp. Fiz. Nauk **173**, 113 (2003) [Phys. Usp. **46**, 105 (2003)].
21. L. N. Bulaevskii, A. I. Buzdin, and S. V. Panjukov, Solid State Commun. **44**, 539 (1982).
22. E. A. Demler, G. B. Arnold, and M. R. Beasley, Phys. Rev. B **55**, 15 174 (1997).
23. F. S. Bergeret, A. F. Volkov, and K. B. Efetov, Phys. Rev. B **64**, 134506 (2001).
24. F. S. Bergeret, A. F. Volkov, and K. B. Efetov, Phys. Rev. B **65**, 134505 (2002).
25. M. Yu. Kupriyanov, Sov. J. Low Temp. Phys. **7**, 342 (1981).
26. M. Yu. Kupriyanov, K. K. Likharev, and V. F. Lukichev, Sov. Phys. JETP **56**, 235 (1982).
27. G. Eilenberger, Z. Phys. **214**, 195 (1968).
28. M. V. Kalenkov, H. Kloos, and A. D. Zaikin, private communication.